

# Second Order Edge-preserving Regularized Functional for Recovering Discontinuous Phase Maps in Fringe Patterns with Carrier

Carlos A. Galvan<sup>a</sup> and Mariano Rivera<sup>b</sup>

<sup>a</sup>Centro Nacional de Metrologia, Apdo. Postal 1-100 Centro, Queretaro, Qro., 76000, Mexico

<sup>b</sup>Centro de Investigacion en Matematicas, Apdo. Postal 402, Guanajuato, Gto., 36000, Mexico

<sup>a</sup>cgalvan@cenam.mx, <sup>b</sup>mrivera@cimat.mx

## ABSTRACT

This paper proposes a robust method for computing discontinuous phase maps. The proposed algorithm is based on the minimization of a edge-preserving regularized cost functional. We use a robust regularized potential based on the paradigm of the Plate with Adaptive Rest Condition (PARC). Our algorithm computes the phase from fringe patterns with discontinuities on the fringe pattern due to steps on the phase and changes on the illumination component. The method is presented in the context of calibrating Gauge Blocks by interferometric method. The performance of the method is demonstrated by numerical experiments on both synthetic and real data.

**Keywords:** Fringe analysis, Gauge blocks, Edge preserving regularization, Phase recovery.

## 1. INTRODUCTION

We present a general algorithm for computing discontinuous phase map, and illumination conditions discontinuous too. This kind of interferograms can be obtained in Gauge Block calibration process by interferometry. This task is described in section 2. The proposed model was design for fringe patterns with a carrier signal which frequency is known (or can be computed) with good precision. The estimation error of the carrier frequencies introduces in the computed phase a constant slope.

This paper is organized as follows. In Section 2 we describe the problem that we use like reference framework: the computation of the phase map from a fringe pattern with carrier frequency. This kind of interferograms can be obtained in the calibration of Gauge Block (GB) by interferometric means. In section 3 is presented a brief review to regularization based on PARC potentials. In our knowledge, the only second order edge preserving regularization method that deal naturally with first order discontinuities, this means, model support variations with a constant slope. In section 4, we present a SPARC model based on a regularization functional proper for fringe pattern with carrier analysis, this model includes illumination parameters estimation for a complete fringe pattern analysis, this section describes a minimization algorithm for that functional. Finally, in section 5 the performance of the methods is demonstrated by both synthetics and real interferograms obtained from CENAM Gauge Block interferometer .

## 2. STATEMENT OF THE PROBLEM

The task of GB calibration by interferometric methods is an important activity performed by primary metrology laboratories. Some of these laboratories are the National Institute of Standards and Technology (NIST) in the United States, the National Research Council in Canada, the National Physics Laboratory in the UK, or the Centro Nacional de Metrologia (CENAM) in Mexico.

The GB are first step on the dissemination chain of the length standard: the meter; only the national's length standard is determined with a higher precision. This high precision task is archived by using interferometers (previously calibrated with respect the national length standard). The GB calibrated in this way, are used as standards in calibration of others GB, devices calibration with less precision as coordinate measuring machines. This paper concerns about the GB calibration performed by interferometric techniques. Particularly, we deal the development of an algorithm for the phase retrieval of a single interferogram of the GB. In figure 1, we show two interferograms corresponding to GB of different material; panel

(a) shows the corresponding interferogram for a tungsten-carbide GB and panel (b) to a steel GB. Fringe patterns shown in figure 1 were obtained from CENAM Gauge Block Interferometer, this one is a commercial instrument, which uses a Twyman-Green interferometer with two different wavelength lasers (633nm and 540 nm wavelength lasers). Gauges to be measured are wrung onto a lapped reference plate and positioned in the interferometer to provide a set of tilt fringes across the gauge and plate. The fractional displacement of the fringes on the gauge relative to those on the plate, known as the fringe fraction, is estimated. If the gauge length has been previously determined within  $\pm 1,5 \mu\text{m}$  of the true length the method of exact fractions can be used to compute a better estimate of the gauge length from observed fringes fractions<sup>5</sup>.

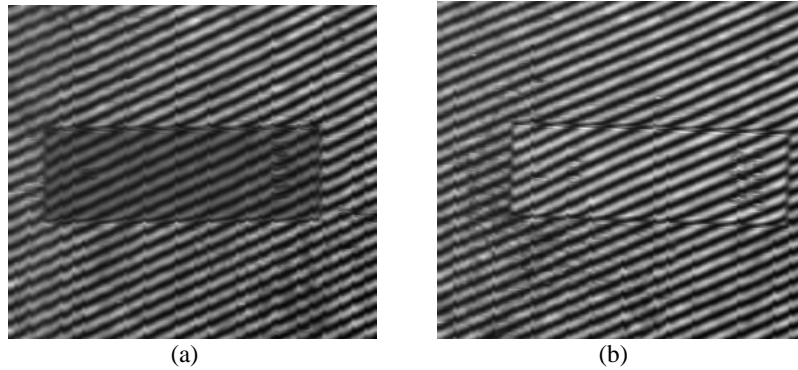


Figure 1. Interferograms obtained from CENAM Gauge Block Interferometer for two different kind of gauge block. a) a tungsten carbide gauge block wrung on a steel plate and the second section shows a steel gauge block on a steel plate.

Interferograms shown in figure 1, can be represented by the observation model (or direct model):

$$g_r = a_r + b_r \cos(f_r), \quad (1)$$

where  $r=[x,y]^T$  represents the position of the pixel  $r$  in the regular lattice  $L$ ,  $a$  is the illumination background,  $b$  is the contrast, and  $f$  can be expressed as

$$f_r = \omega^T r + \phi_r; \quad (2)$$

where  $\omega=[\omega_x, \omega_y]^T$  is the spatial carrier frequency, and finally  $\phi$  is the phase. Given the condition of the experimental setup, we can make the followings considerations:

- (a) The illumination components (background and contrast) are piecewise smooth because the difference of material composition of the elements in the scene.
- (b) The phase is piecewise smooth because the gauge block presence.
- (c) The carrier frequencies are constant, but their precise value are unknown, and they were chosen in a way such that there are not closed fringes in the scene.

The task is to compute phase map  $\phi$  for each pixel in the fringe pattern, but sometimes is useful to have an estimation of brightness, contrast and discontinuities maps. In last decade, several authors have proposed several methods using regularization techniques<sup>2</sup> like quadrature filters, adaptive quadrature, etc. But most of them do not include a carrier frequency on interference equations; even the illumination effects are taken off the analysis.

In resume our goal is propose a model to find fractional displacement from fringe pattern in GB calibration task. In order to solve this inverse problem, we proposed to minimize a regularized energy functional. In the regularization framework, the solution is computed as the minimum of an energy functional<sup>8,9</sup> of the general form

$$U(a, b, \phi) = D(a, b, \phi; g) + \lambda R(a, b, \phi), \quad (4)$$

where the first term,  $D$ , is known as the data term and promotes fidelity of the computed variables to the observed data. The second term,  $R$ , codifies the *a priori* information about the solution. Generally is expressed as a term that promotes smoothness of the solution.

### 3. REGULARIZATION USING PARC POTENTIALS

The data term is expressed with based in the observation model given in Eq. (1) :

$$D(a, b, \phi; g, \varpi) = \sum_{r \in L} (a_r + b_r \cos(\varpi^T r + \phi_r) - g_r)^2 . \quad (5)$$

Regularization term must be expressed in a form such that imposes a penalty for violation *a priori* assumption expressed in (3). This term can be expressed in general for as

$$R(t) = \sum_{r \in L} \sum_{s \in N_r} \rho(t_r, t_s) , \quad (6)$$

where  $N_r$  is the set of neighbours pixels to  $r$ . The form of the neighbourhood will be defined in next section. The selection of the right regularization potential function  $\rho$  is the key point to obtain good results. Standard regularization potentials correspond to set  $\rho(t) = t^2$ . It is well known that this potential over-smooths the edges in the scene. In other hand, edge-preserving regularization methods based on robust potentials, are for example  $\rho(t) = 1 - \exp(-t^2)$ , allows to deal with steps on phase or illumination. However, error in the estimation of the carrier frequencies produce that the robust potentials introduce new edges in zones with constant gradient (known as the "staircase" effect). The carrier frequencies depends of the relative tilt of the reference mirror and are estimated with a limited accuracy (for instance, the method suggested by Huntley based on Fourier Transform<sup>6</sup>). That conducted us to use the second order edge preserving potentials recently reported by Rivera and Marroquin<sup>1,10</sup>, so called plates with adaptive rest condition (PARC) potentials. PARC potentials have the advantage that deal with ramps (regions with smooth variations in the intensity gradient) and first order discontinuities (steps). This represents a significant advantage over the half-quadratic plate model based on robust potentials<sup>9</sup>.

In this paper we use a potential of the kind of analogical line process (PARC-AL). Specifically, we implement the second order edge-preserving potentials with explicit line process:

$$\rho_{\text{parc}}(f, l) = ((f_q - f_r)l_{qr} - (f_r - f_s)l_{rs})^2 + \mu[l_{qr}^2 + l_{rs}^2] , \quad (7)$$

where cliques of three pixels  $\langle q, r, s \rangle$  are used. This cliques represent triads of pixels in horizontal, vertical and diagonal positions, see figure 2.

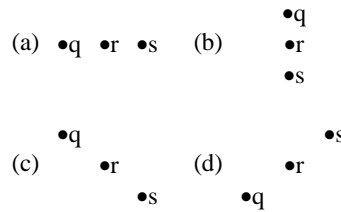


Figure 2. Cliques of pixels in positions: (a) horizontal, (b) vertical and (c) and (d) diagonal.

Potential given in Eq. (7) has the following properties:

1. It is close to zero for small values of  $|\Delta^+ f_r + \Delta^- f_r|$
2. For large values of  $|\Delta^+ f_r + \Delta^- f_r|$  becomes a classical robust potential. This is, grows to an slow rate than the quadratic potential.
3. For small values of  $|\Delta^+ f_r|$  and large values of  $|\Delta^- f_r|$ , the potential is robust for the large value. Similar behavior of the case of large values of  $|\Delta^+ f_r|$  and small values of  $|\Delta^- f_r|$ .

In next section, we present the complete functional for phase recovery with second order discontinuities.

#### 4. EDGE PRESERVING FUNCTIONAL FOR FRINGE ANALYSIS BASED ON PARC POTENTIALS

In fringe patterns we are considering, if a discontinuity on the illumination components occur, it coincides with the phase discontinuities (see figure 1). Therefore, the potential function must to couple the steps on illumination with the steps on phase by means of a single edge detector field  $l$ . The functional we proposed is

$$U(a, b, \phi, l) = \sum_{r \in L} (a_r + b_r \cos(\omega^T r + \phi_r) - g_r)^2 + \sum_{\langle q, r, s \rangle \in L} \left\{ \alpha \left( (a_q - a_r)l_{qr} - (a_r - a_s)l_{rs} \right)^2 + \beta \left( (b_q - b_r)l_{qr} - (b_r - b_s)l_{rs} \right)^2 + \gamma \left( (\phi_q - \phi_r)l_{qr} - (\phi_r - \phi_s)l_{rs} \right)^2 + \mu [l_{qr}^2 + l_{rs}^2] \right\} \quad (8)$$

where the positive regularization parameters,  $\alpha$ ,  $\beta$ ,  $\gamma$  and  $\mu$ , controls the relative contribution of each term to the total cost. In order to minimize functional  $U(a, b, \phi, l)$  we use an alternated minimization scheme. This corresponds to an iterative four steps algorithm:

Given an estimation for  $\omega$ , set the initial guess  $a = 1$ ,  $b = 1$  and  $l = 1$ , and to compute a initial phase  $\phi^0$  (this is clarified in the next paragraph) for all the pixels  $r$  in  $L$ .

1. Compute  $\phi$  as the minimum of  $U$ , keeping  $a$ ,  $b$  and  $l$  fixed.
2. Compute  $a$  as the minimum of  $U$ , keeping  $\phi$ ,  $b$  and  $l$  fixed.
3. Compute  $b$  as the minimum of  $U$ , keeping  $a$ ,  $\phi$  and  $l$  fixed.
4. Compute  $l$  as the minimum of  $U$ , keeping  $a$ ,  $b$  and  $\phi$  fixed.

Note that steps 2, 3 and 4 correspond to perform a quadratic minimization that can be performed by using standard minimization algorithm as gradient descent or conjugate gradient. However, because of the cosine function, the minimization over the phase  $\phi$  leads to the solution of a non-linear equation system. For solving the non-linear system, our strategy consists on estimate a good initial guess of the phase  $\phi^0$  (corresponding to the computed with a standard fringe analysis algorithm) and then to use a gradient descent algorithm. If the initial guess for the phase were the homogeneous map equal to 0, the algorithm computes the wrapped phase and additional edges will appear at the sites where the phase is wrapped.

#### 5. RESULTS

This section describes results obtained with both synthetic and real data. The first set of experiments consist on the analysis of one dimensional synthetic data, second set of experiments correspond to the analysis of one-dimensional real data, and finally, last set of experiments was conducted on the complete two-dimensional fringe pattern. The real data corresponds to the obtained from the TESA Gauge Block Interferometer at CENAM.

Figure (3-a) shows, a signal with synthetic data (values of phase and illumination elements  $a$  and  $b$ ) generated with the direct observation model given in Eq (1) and setting:

$$\phi_x = \begin{cases} 1,2 + 0,005x & 97 \leq x \leq 165 \\ 0,2 + 0,005x & \text{other wise} \end{cases}, \quad a_x = \begin{cases} 0,6 & 97 \leq x \leq 165 \\ 1 & \text{other wise} \end{cases}, \quad \text{and} \quad b_x = \begin{cases} 0,5 & 97 \leq x \leq 165 \\ 0,9 & \text{other wise} \end{cases}.$$

Then the one-dimensional fringe pattern was generated using a known frequency and by adding Gaussian noise. Figure 3-b shows results obtained using the propose method using the real carrier frequencies. As one can see, phase, illumination components and edges are computed correctly.

Second set of experiments corresponds to use real data. Results obtained are shown in figure 4. Panel 4-(a) shows data from a fringe pattern image column obtained from TESA interferometer, in this example a tungsten-carbide GB was wrung on a steel reference plate. One can observe steps on phase an illumination components. The results, computed with the proposed algorithm, are shown in panel 4-(b). We can observe, in region of the computed the phase map corresponding to the GB, a small tilt that may result of an incorrect wrung process of the GB on the reference plate.

Finally, in figure 5, we shows the result of the analysis of a two dimension fringe pattern, The edges map, panel 5-(d) allows us to compute the central point of the block, where, according with international standards is located point to calibrate.

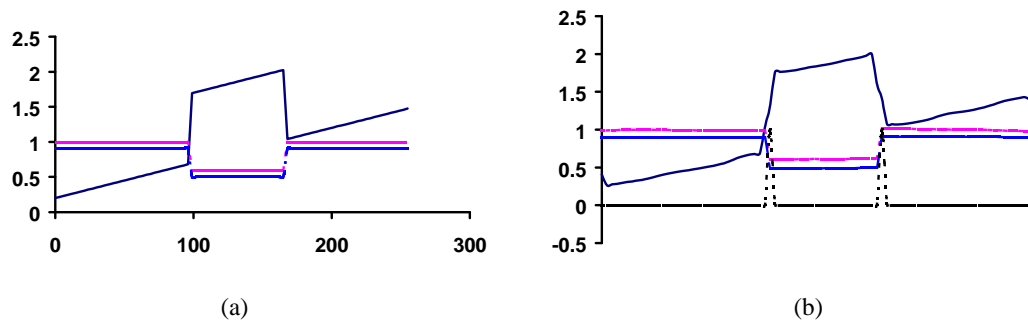


Figure 3. One dimension signal. a) Synthetic data for phase values (continuous line), background illumination values (point line) and contrast (points). b) Recovery data with the PARC regularized functional, one can observe the right edge detection. Original model was added with white noise signal with a standard deviation 0.5

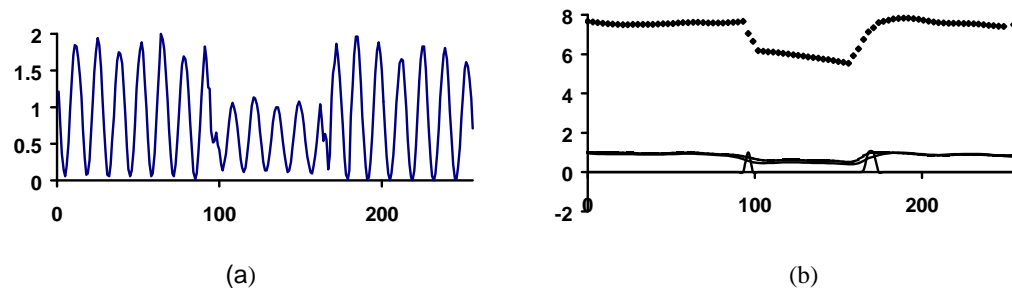


Figure 4. Real data from TESA interferometer. a) Observed row data in TESA interferometer with red laser.. b) Recovery data using PARC model, phase map (signal in 6-8 interval), illumination elements (values around 1), and edges.

## 6. CONCLUSIONS

We presented a regularization model to process fringe patterns with carrier in order to recovery phase map, and illumination parameters according with the interference equation. This method supports edge detection so discontinuities on phase map are correctly detected and managed. Due to the algorithm is based on a second order edge detection regularization potential, the method can detect smooth zones with almost constant value or almost constant gradient. The performance of method was illustrated in numerical experiments on both synthetic data with real data. The real test data correspond to the fringe patterns obtained from a Gauge Block Automatic Interferometer used at Centro Nacional de Metrología (CENAM) (primary metrology laboratory in Mexico). Future work will focus in the investigation of minimization algorithm that reduce the analysis time. Currently, the computational time, using a 300Mhz PC Pentium II, is around 6 hours to solve two-dimensional phase maps while in the one-dimensional task is around 20 seconds.

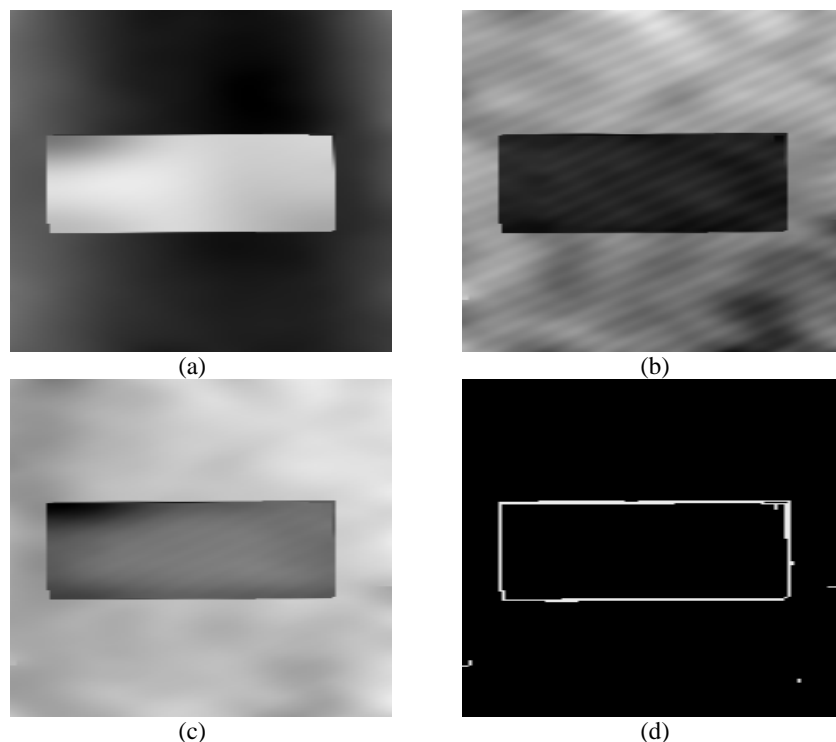


Figure 5. Recovery data from a two dimension fringe pattern using PARC model. a) phase map b)background illumination c) contrast image map d)edge map.

## REFERENCES

1. M. Rivera, J.L. Marroquín, *The adaptive rest-condition spring system: and edge-preserving regularization technique* in Procc. of the IEEE Int. Conf. on Image Processing, IEEE Signal Processing Society, Vancouver, BC, Canada, Sept. 2000.
2. J.L. Marroquin, M. Rivera, S. Botello, R. Rodríguez-Vera and M. Servín, *Regularization methods for processing fringe-pattern images* Applied Optics, Vol 38, No. 5, pp 788-795, 1999
3. D. Malacara, *Optical Shop Testing* Second Edition, John Wiley and Sons, 1992.
4. P. Carre, *Installation et Utilisation du Comparateur Photoelectrique et Interferentiel du Bureau International des Poids des Mesures* Metrologia 2, vol 13, 1966.
5. D.J. Pugh, K Jackson, "Automatic gauge block measurement using multiple wavelength interferometer," SPIE vol 656 Contemporary Optical Instrument Design, Fabrication and Testing (1986)
6. J.M. Huntley, "An image processing system for the analysis of speckle photographs", J. of Physics E: Sci. Instrum. Vol. 19, 1986
7. Galván C. "Análisis de franjas usando regularización con potenciales con condición de reposo adaptable". Tesis de maestría en ciencias de la computación y matemáticas industriales, CIMAT, 2000
8. J.L. Marroquin, S. Mitter and T. Poggio, "Probabilistic Solution of Ill-Posed Problems in Computational Vision, " Journal of the American Statistical Association, vol 82, No. 397, pp 76-89, 1987.
9. D. Geman and G. Reynolds, "Constrained restoration and recovery of Discontinuities," IEEE Transactions on Pattern Analysis and Machine Intelligence, vol 14, pp 367-383, 1992.
10. Rivera, M., Marroquin, J.L.: Adaptive Rest Condition Potentials: Second Order Edge-Preserving Regularization, In Proc. European Conference on Computer Vision, ECCV 2002, Springer-Verlag, Copenhagen, Denmark, May (2002)